Article

Impact of Electric Vehicles on Energy Efficiency with Energy Boosters in Coordination for Sustainable Energy in Smart Cities

Pawan Kumar [1,*], Srete Nikolovski [2,*], Ikbal Ali [3], Mini S. Thomas [3] and Hemant Ahuja [4]

1   Electrical and Instrumentation Engineering Department, Thapar Institute of Engineering and Technology, Patiala 147004, India
2   Power Engineering Department, Faculty of Electrical Engineering, Computer Science and Information Technology, J. J. Strossmayer University of Osijek, K. Trpimira 2B, HR-31000 Osijek, Croatia
3   Department of Electrical Engineering, Faculty of Engineering & Technology, Jamia Millia Islamia, New Delhi 110025, India
4   Department of Electrical and Electronics Engineering, Ajay Kumar Garg Engineering College, Ghaziabad 201009, India
*   Correspondence: pawanror@gmail.com (P.K.); srete.nikolovski@ferit.hr (S.N.)

Abstract: The use of electric vehicles (EVs) has recently increased in a smart city environment. With this, the optimal location of the charging station is a great challenge and, hence, the energy efficiency performance (EEP) of an electrical system is important. Ideally, the EEP is realized through passive energy boosters (PEBs) and active energy boosters (AEBs). PEBs require no external resources, and EEP is achieved through altering the network topology and loading patterns, whereas, in AEBs, integrating external energy resources is a must. The EEP has also become dynamic with the integration of an energy storage system (ESS) in a deregulated environment. Customer energy requirement varies daily, weekly, and seasonally. In this scenario, the frequent change in network topology requires modifying the size and location of AEBs. It alters the customers' voltage profile, loadability margin, and supply reliability when the EV works differently as a load or source. Therefore, a comprehensive EEP analysis with different probabilistic loading patterns, including ESS, must be performed at the planning stage. This work uses a harmony search algorithm to evaluate EEP for AEBs and PEBs, in coordination, when ESS works as a load or source, at four locations, for customers' and utilities' benefits.

1. Introduction

Technological development paves the way to modernization with significant enhancements in energy consumption, where electricity plays a crucial role. In this scenario, sustainable energy is the primary requirement for a sustainable society. Though energy resources are depleting day by day, it is necessary to explore the ever-best approach for energy efficiency while generating, distributing, and utilizing electricity. In the current scenario, societal development mainly depends upon the availability of energy resources. Conversely, the consumers' energy demand has grown unexpectedly, and agencies are working tirelessly to explore various energy resources. The availability of the resources is limited. Therefore, the smart systems for energy efficiency in generation, distribution, and utilization can be considered alternatives to the resources for sustainable energy and society.

A smart energy system has two aspects: namely, (a) realization of technical parameters for energy efficiency and (b) bidirectional communication with power components for their control and monitoring. The first part is more critical to developing a smart infrastructure for operation and control. In the present scenario, the loading pattern varies with the state

of the economy and system voltage profile. The involvement of smart devices encompasses power electronic devices and converters; the loading pattern has become highly non-linear and needs to be managed on an hourly basis [1]. It further alters the loadability margin and reliability of power supply, at respective load points, during power delivery. However, in recent years, the technological evolution in electric vehicles has introduced a new scope of research for energy efficiency in smart energy systems.

Further, in a smart city environment, the EEP of a distribution system depends upon several parameters. It changes with the representation of loads, network topology, integration of DGs and shunt capacitors, and the implementation of various DSM approaches during power delivery. In addition, in recent years, the integration of EVs has evolved the new research challenges for energy efficiency. In this work, EEP is realized with and without external energy resources to benefit utility and consumers. The approach for EEP without external energy resources is defined as a passive energy booster, whereas the approach for EEP with external energy resources is the active energy booster. In the past, the researchers have presented several approaches, with slight modifications, based on PEBs and AEBs, exclusively. From consumers' perspectives, in this work, the EEP is realized by PEBs and AEBs in coordination with ESS, and a comprehensive evaluation is presented based on several operating parameters.

Several approaches exist for the EEP of the distribution system, and using single and multi-objective functions, with line losses, are a significant concern. Ideally, it is beneficial for utilities, whereas it has little significance in consumers' interests. Ali et al. [2] have presented several indices-based approaches for the comprehensive evaluation of EEP of the distribution system. Here, the authors considered different combinations of the load models, and EEP is realized with and without the integration of external energy resources exclusively. A heuristic approach is developed, and the weightage of different indices is varied to show their effects on EEP. However, in this approach, the loads are represented with fixed weightage to the particular load class or type, as well as under fixed weightage to the energy parameters. As an extension to the method presented in [2], it is required to evaluate the system performance for a possible number of customers, as well as the reliability of power supplies under different probabilistic loading patterns, including ESS.

Authors in [3,4] have developed a heuristic approach, for improving a system's voltage profile and EEP, by considering a different objective in optimization that allows the more significant number of customers to be supplied at a particular time instant. However, authors in [5] have developed the DSM approach under different loads, such as electric vehicles, mobile charge, and energy storage devices, for smart grid systems with fixed network topology. Habeeb et al. [6] have presented the energy management system, with local generation and energy storage, for domestic applications. Conversely, in [7], authors have developed schemes for the operation of different power equipment throughout the day. The real-time implementation of these approaches tends to alter the loading patterns hourly. In this scenario, the representation of loads in power system operation and stability studies plays an important role. Bin et al. [8] have presented a multi-objective optimization problem in a hybrid microgrid environment, where power generation from the PV system, windmills, and ESS is simulated using fuzzy techniques. Here, the authors have also considered the static loading patterns, and no emphasis has been laid on the voltage dependency of loading patterns during a change in network topology. In [9], the integration of these power generating systems has been simulated with DSM, for an agriculture farm, to reduce the energy demand of the power grid.

With the implementation of the DSM approach, the load demand was found to be varying significantly in [10], where the energy demand of the commercial building is evaluated for the intensification of energy efficiency. However, Asrari et al. [11] and Dorostkar et al. [12] have presented the impact of DER on the electrical system during network reconfiguration for EEP. Similarly, in [13,14], the reconfiguration is performed to improve the reliability of supplying power, with a vehicle, to grid and DG allocation in an active distribution system, respectively. Conversely, Fu et al. [15] revealed that the

reconfiguration is limited due to switching loss. Therefore, it requires development of a timeframe for a particular configuration for the capacity enhancement of existing networks. Ali et al. [16] have also presented the reconfiguration, in the presence of ESS, considering static loads. In [17], reconfiguration is performed under an unbalanced distribution system to coordinate voltage regulators and renewable resources. Song et al. [18] considered the voltage volatility due to DER, and reconfiguration is performed to minimize it, but in [19], DG allocation is presented in the presence of ESS for energy performance.

Naguib et al. [20] conferred that environmental uncertainty can affect the system performance during reconfiguration and DG allocation. Cattani et al. [21] addressed the distribution system planning by using reconfiguration, and in [22], an AC-DC hybrid distribution system is developed for the customer's energy management. Takenobu et al. [23] presented the annual energy consumption, based on the reconfiguration of the distribution system, under different operating conditions. This allows system operation flexibility, and it benefits both the customer and the utility. Conversely, Arsari et al. [24] presented a new framework of DG allocation, based on time management, hourly—ahead of the system's decision making—to reduce the necessity of reconfiguration. In [25], the authors emphasize the short-term improvement in the voltage profile when using network reconfiguration. However, in [26,27], the process of reconfiguration is highlighted, and heuristic approaches are developed for single or multilevel switching operations, whereas in [28–30], network reconfiguration is performed for loss reduction under a fixed loading scenario.

The above literature has revealed that network reconfiguration and DG allocation play crucial roles in the EEP of an electrical system. However, in these approaches, the impact of ESS on EEP has not been considered; instead, they focused on the conventional approach of network reconfiguration and DG allocation. These approaches can be realized in two ways: namely, (i) the approaches in which no external energy resource is required to improve the EEP and (ii) the approach in which external source is a must to improve the EEP. The former is called a passive energy booster, and later, is an active energy booster. Further, in recent years, the new type of load, featured with ESS, can be recognized as a dynamic load since it can work as a load or source, while charging or discharging, respectively.

The performance of the electrical power system with ESS has been presented in [31–33]. However, in these studies, the representation of physical loads and network reconfiguration have not been considered; instead, results are demonstrated under constant power loads only. However, in smart energy infrastructure, the voltage dependency of these loads cannot be ignored. An extensive review presented in [34] has emphasized the need of ESS for a sustainable microgrid. Considering the above facts, this work intended to develop a probabilistic loading pattern for the comprehensive evaluation of EEP of the electrical systems in a smart energy system's environment. Moreover, in this work, DG allocation and network reconfiguration are performed, in coordination, under different loading patterns, including ESS, which is beneficial for the customer and utilities in a sustainable city and society.

The organization of the paper is as follows: The extensive literature review is presented under the introduction in Section 1. The mathematical formulations, with operating constraints, load modeling, and EEP parameters, are described in Section 2. However, Section 3 presents a detailed description of the harmony search algorithm, whereas Section 4 presents the procedural steps involved in the proposed algorithm. Section 5 describes the test system and the case study cases. Section 6 presents the test results and discussion, and finally, the results and findings are concluded in Section 7.

2. Mathematical Formulations for Energy Efficiency

2.1. Problem Formulation

With the involvement of smart devices in energy systems, the operation and control has become fast. As a result, it has improved the decision-making capacity under the frequent change in operating conditions for energy efficiency, which involves the reduction in power loss, improvement in voltage profile, and loadability margin—exclusively or in

coordination—with certain weightage of each parameter. However, the change in working conditions may compromise one parameter over another. In this scenario, the primary function of PEBs and AEBs is to deal with the constraints, such as active and reactive power demand, voltage limits, line capacity, and network radiality. Therefore, the optimization problem is formulated as follows:

$$\text{Minimize} \rightarrow f(x) \tag{1}$$

The above problem is subject to the following constraints:

a.   *Active and reactive power limit:* The algebraic sum of all the generations, power demands, and power losses should be zero, and it is defined as:

$$\sum_{i=1}^{n} P_{Gi} - \sum_{i=1}^{n} P_{Di} - \sum_{i=1}^{n} P_{Li} = 0 \tag{2}$$

$$\sum_{i=1}^{n} Q_{Gi} - \sum_{i=1}^{n} Q_{Di} - \sum_{i=1}^{n} Q_{Li} = 0 \tag{3}$$

Here, in (2) and (3), the P_{Gi} and Q_{Gi} are the generated power at the *i*th node, P_{Di} and Q_{Di} are the demands at the *i*th node, and P_{Li} and Q_{Li} is the power losses beyond *i*th node.

b.   *Voltage limit:* The PEBs and AEBs are responsible for improving the system voltage profile. However, PEBs can improve up to a certain extent, whereas AEBs can improve the voltage profile even beyond 1.0 pu. Therefore, voltage limit restrains the overcompensation due to AEBs, and it is defined in (4):

$$V_{i,min} \leq V_i \leq V_{i,max} \tag{4}$$

c.   *Capacity limit:* In power distribution, the lines have their capacity to transfer power and, hence, the loadability. The line capacity is usually evaluated with current limits, and the maximum load that can be connected at a particular node is defined with kVA loading. These limits are described in (5).

$$\left.\begin{array}{c} I_i < I_{i,\ max} \\ kVA_i < kVA_{i,\ max} \end{array}\right] \tag{5}$$

d.   *Network radiality limit:* A distribution system is generally operated as radial to coordinate protecting devices. The branches are arranged in a downward stream. In a set of branches, the index value k_{ij} is equal to '1' for all connected branches between the '*i*th' and '*j*th' nodes; otherwise, it is zero if that branch is considered as a tie-line in the configuration. In a radial network,

$$kij = 1 \rightarrow \rightarrow \text{ for all connected branches}$$

$$kij = 0 \rightarrow \rightarrow \text{ for tie-lines}$$

Therefore, for network radiality the following is to be satisfied.

$$\sum k_{ij} = n - 1 \tag{6}$$

Here, in (6), 'n' is the total number of nodes in a radial path, including the substation.

e.   *State of charge limit:* An energy storage system (ESS) in electrical power distribution can work as a load, as well as an energy resource, depending on its state of charge during operation. ESS below its lower limit of SOC tends to work as load, whereas it can meet load demand under peak loading conditions when SOC is above the prescribed limit.

$$SOC_{b,min} \leq SOC_b < SOC_{b,max} \tag{7}$$

    f.   *AEB's limit:* The external DGs are the source of AEBs. If AEBs are operated below their minimum prescribed limit, they become uneconomical. The lower limit is taken as 0.3 times of its full capacity in this work. Therefore, the following limits are imposed for AEBs for the energy-efficient operation of the power system.

$$0.3 \times AEB_{i,max} \leq AEB_i < AEB_{i,max} \tag{8}$$

2.2. Energy Efficiency Analysis

In the deregulated competitive energy market, the energy efficiency is not limited to a mere single parameter, such as the reduction in power loss. Rather, it depends upon several other parameters, such as time of operation, loading patterns, state of the economy, environmental conditions, and the number of customers to be supplied, i.e., loadability limit, voltage profile at the customer end, reliability of supplying power, as well as the quantity and quality of supplying power. To improve the EEP, utilities usually implement energy boosters during operation. These energy boosters can be classified as PEBs and AEBs. The effect of various PEBs and AEBs on the EEP is summarized in Table 1.

Table 1. Parameters for energy efficiency performance.

S. No.	Parameters	Significance in EEP
1	kW demand (Ps_i)	The integration of PEBs and AEBs improves the voltage profile, altering the loading pattern.
2	kVAr demand (Qs_i)	The reactive power flow in the system directly affects the voltage profile. The higher the reactive power lower will be the voltage and hence the poor energy efficiency.
3	kVA demand (Ss_i)	The number of customers to be supplied depends upon the kVA rating of transformer at load point.
4	Node voltage profile (V_i)	The loads are voltage-dependent, and hence, the voltage profile can alter the loading pattern and the operating efficiency of the connected loads.
5	Loadability index (f_{si})	Loadability margin limits the maximum number of customers supplied at a particular node.
6	Power loss (P_L)	PEBs and AEBs reduce the power loss by improving voltage profile and local generation.
7	Margin of Reliability (MR)	The reliability of supplying power is influenced by the possible number of consumers, voltage limit, and thermal limit. The PEBs and AEBs improve these aspects and hence the reliability.

2.3. Load Representation and Modeling

Practical loads are the combination of several types of loads having different characteristics [35]. The operating characteristics of these loads may change with time and the system voltage profile. Depending on their voltage profile sensitivity, loads are classified as residential, commercial, and industrial loads. Conversely, the operating characteristics can be represented as constant power, constant current, and constant impedance for individual loads. In practice, these loads act together, and therefore, it is required to consider the various combinations of different load classes and types, as shown in Table 2.

Table 2. Load type and load class with their voltage exponents.

Load Type	Voltage Exponents		Load Class	Voltage Exponents	
	α	β		α	β
Constant power	0	0	Industrial	0.18	6.0
Constant current	1	1	Commercial	0.99	3.5
Constant impedance	2	2	Residential	1.2	2.9

In this work, based on the above representation, the loads are modeled as follows:

a. *Load model-1 (LM-1):* In LM-1, the load at each node is considered to be a constant power type and represented as

$$P_i = a * P_{i0} \left[\frac{V_i}{V_{i0}} \right]^{\alpha}$$
$$Q_i = a * Q_{i0} \left[\frac{V_i}{V_{i0}} \right]^{\beta} \tag{9}$$

b. *Load model-2 (LM-2):* In LM-2, the loads are considered as the combinations of various load types, such as constant power, constant current, and constant impedance loads, and it is represented as

$$P_i = P_{i0} \left(a \left[\frac{V_i}{V_{i0}} \right]^{\alpha_1} + b \left[\frac{V_i}{V_{i0}} \right]^{\alpha_2} + c \left[\frac{V_i}{V_{i0}} \right]^{\alpha_3} \right)$$
$$Q_i = Q_{i0} \left(a \left[\frac{V_i}{V_{i0}} \right]^{\beta_1} + b \left[\frac{V_i}{V_{i0}} \right]^{\beta_2} + c \left[\frac{V_i}{V_{i0}} \right]^{\beta_3} \right) \tag{10}$$

c. *Load model-3 (LM-3):* In LM-3, the loads are considered as the combinations of various load classes, such as residential, commercial, and industrial loads, and it is represented as

$$P_i = P_{i0} \left(x \left[\frac{V_i}{V_{i0}} \right]^{\alpha_1} + y \left[\frac{V_i}{V_{i0}} \right]^{\alpha_2} + z \left[\frac{V_i}{V_{i0}} \right]^{\alpha_3} \right)$$
$$Q_i = Q_{i0} \left(x \left[\frac{V_i}{V_{i0}} \right]^{\beta_1} + y \left[\frac{V_i}{V_{i0}} \right]^{\beta_2} + z \left[\frac{V_i}{V_{i0}} \right]^{\beta_3} \right) \tag{11}$$

In (10), voltage exponents $\alpha_1 = \beta_1 = 0$, $\alpha_2 = \beta_2 = 1$, and $\alpha_3 = \beta_3 = 2$, as well as 'a', 'b', and 'c' are the fractional contributions in the LM-2. Conversely, in (11), the voltage exponents $\alpha_1 = 0.18$, $\beta_1 = 6.0$, $\alpha_2 = 0.99$, $\beta_2 = 3.5$, and $\alpha_3 = 1.2$, $\beta_3 = 2.9$, as well as 'x', 'y', and 'z' are the fractional contributions in LM-3. In various LMs, the fraction 'a', 'b', 'c' and 'x', 'y', 'z' are obtained using (21), where it varies at random as a function of probabilistic constant factor (PCF).

Considering the above formulation, the node voltage and loadability are calculated using equivalent radial network between two nodes, as shown in Figure 1:
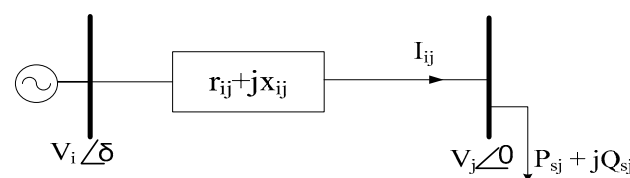
Figure 1. Representation of radial network between two nodes.

Let the receiving-end power factor angle (θ), sending-end voltage angle (δ), and $\Psi = \theta + \delta$, so the following equations can be written:

$$V_i \cos \Psi = V_j \cos \theta + I_{ij} r_{ij} ; \tag{12}$$

$$V_i \sin \Psi = V_j \sin \theta + I_{ij} x_{ij} ; \tag{13}$$

$$V_i^2 = \left(V_j cos\theta + I_{ij}r_{ij}\right)^2 + \left(V_j sin\theta + I_{ij}x_{ij}\right)^2 \tag{14}$$

Equation (14) can be written as (15), in terms of load demand, as follows:

$$V_i^2 = V_j^2 + 2r_{ij}P_{sj} + 2x_{ij}Q_{sj} + \left(r_{ij}^2 + x_{ij}^2\right)\left[\frac{P_{sj}^2 + Q_{ij}^2}{V_j^2}\right] \tag{15}$$

Further re-arranging (15) gives receiving-end voltage, represented, as follows, by (16):

$$V_j = \left[\frac{V_i^2}{2} - \left(r_{ij}P_{sj} + x_{ij}Q_{sj}\right) \pm \left[\left\{\frac{V_i^2}{2} - \left(r_{ij}P_{sj} + x_{ij}Q_{sj}\right)\right\}^2 - \left(r_{ij}^2 + x_{ij}^2\right)\left(P_{sj}^2 + Q_{sj}^2\right)\right]^{\frac{1}{2}}\right]^{\frac{1}{2}} ; \tag{16}$$

The loadability limit is the maximum volt-ampere capacity of a radial feeder. Equation (16), for receiving-end node voltage, is used to find the loadability limit. The following inequality constraint is to be satisfied for the feasible solution of (16)

$$\left\{\frac{V_i^2}{2} - \left(r_{ij}P_{sj} + x_{ij}Q_{sj}\right)\right\}^2 - \left(r_{ij}^2 + x_{ij}^2\right)\left(P_{sj}^2 + Q_{sj}^2\right) \geq 0. \tag{17}$$

In order to define the maximum load that can be connected at the respective nodes, the existing load is replaced by $f_{sj} \times (P_{sj} + jQ_{sj})$, and (17) is further modified as a quadratic form of 'f_{sj}'. On solving, it yields

$$f_{sj} = \frac{V_i^2\left[-\left(r_{ij}P_{sj} + x_{ij}Q_{sj}\right) + \sqrt{\left(r_{ij}^2 + x_{ij}^2\right)\left(P_{sj}^2 + Q_{sj}^2\right)}\right]}{2\left(x_{ij}P_{sj} - r_{ij}Q_{sj}\right)^2} \tag{18}$$

Here, 'f_{sj}' is the factor that describes the possible additional load that can be connected at respective nodes before voltage collapse. The value of 'f_{sj}' may vary differently at each node in different configurations. To show the effect of improvement in the voltage profile at respective nodes, in a reconfigured network, the sending-end node voltage is assumed constant for the calculation of loadability factor at any subsequent node. The total power losses in the system are calculated as follows in (19) and (20):

$$P_{LT} = \sum \frac{\left(P_{sj}^2 + Q_{sj}^2\right)}{V_j^2} r_{ij} ; \tag{19}$$

$$Q_{LT} = \sum \frac{\left(P_{sj}^2 + Q_{sj}^2\right)}{V_j^2} x_{ij} ; \tag{20}$$

Equations (19) and (20) show the voltage profile dependence of power losses in the system.

2.4. Probabilistic Loading Patterns (λ) and Cases of Study

In practice, the loading pattern, at a particular node or load point, varies at random, depending on the contribution of a specific load type or class. Equations (21) and (22) describe different loading patterns.

$$\lambda_1 = 1 - PCF \times rand(\,) \tag{21}$$

$$\lambda_2 = \frac{1 - \lambda_1}{2} \tag{22}$$

The value of PCF is operator-dependent, and it can lie between 0 and 1. Here, in (21), the '$0'$' value of PCF means the contribution of 'λ_1' is 100%. It is independent of random function, whereas if PCF > 0, then the loading pattern 'λ_1' will depend upon the random function at that moment, e.g., if PCF is 0.6 and *rand*() is obtained as '1' at any moment, then 'λ_1' will be 40%, which is its minimum value. Similarly, at any other moment, if *rand*() is '$0'$', then the loading pattern (λ_1) will be 100% again. This allows the selection of 'a', 'b', 'c' and/or 'x', 'y', 'z', as well as the corresponding study cases for EEP, of a power distribution system under consideration.

Considering the above formulation, the three different cases of probabilistic loading patterns (PLP), under LM-2 and LM-3, are studied and described in Table 3.

Table 3. PLP under LM-2 and LM-3.

LP	LM-2	LM-3
PLP-1	$a = \lambda_1$ and $b = c = \lambda_2$	$x = \lambda_1$ and $y = z = \lambda_2$
PLP-2	$b = \lambda_1$ and $a = c = \lambda_2$	$y = \lambda_1$ and $x = z = \lambda_2$
PLP-3	$c = \lambda_1$ and $b = a = \lambda_2$	$z = \lambda_1$ and $y = x = \lambda_2$

The selection of 'a', 'b', 'c' and/or 'x', 'y', 'z' is such that

$$a + b + c = 1 \tag{23}$$

$$x + y + z = 1 \tag{24}$$

Therefore, with one component known, the others are equally divided using (22). In LM-2 and LM-3, the fractional values 'x', 'y', and 'z' are the same as 'a', 'b', and 'c'. However, in the analysis, they may be taken differently for the comprehensive evaluation of EEP during power delivery.

2.5. Representation of Energy Storage System

The state of charging and discharging the battery defines the behavior of the energy storage system (ESS) to be worked as a load or source. However, all the ESS may not be fully charged or discharged simultaneously. In this scenario, the representation of the ESS can be modeled with the help of a random distribution function. The ESS, under charging state, works as a load, whereas it will work as a source under discharge state. The modeling of ESS is represented as follows

$$ESS = \pm\, ESS_{in}(1 - PCF \times rand(\,)) \tag{25}$$

In (25), plus and minus represent the behavior of ESS as a load or source, respectively. ESS_{in} is the initial state of ESS that may be fully charged or discharged, as per ESS operation, of load or source. PCF is the probabilistic constant function that is taken as 0, 0.25, and 0.5 for constant power loads. In contrast, for voltage-dependent loads, PCF is taken as 0.4 under different cases of PLPs shown in Table 3. It means, if the value of *rand*() is '1', the minimum or maximum state of charge or discharge of ESS depends upon the PCF.

2.6. Margin of Reliability

During operation, the reliability of supplying power depends upon the connected loads and time of operation. In this scenario, the loading patterns play an important role since, under different circumstances, the behavior of voltage-dependent loads are found to be different, contributing to the reliability of supplying power and energy efficiency at that instant. From [2], it can be observed that the relative value of reliability can exceed the

unity since it is the indexed value. Considering the indexed value of reliability of supplying power, the variation in the margin of reliability (MR) can be evaluated as follows:

$$\%MR = \frac{RI_{base} - RI_{Reconfiguration}}{RI_{base}} \times 100 \tag{26}$$

In (26), the margin of reliability can be plus or minus, depending upon the indexed value of the reliability index (RI), in reconfigured networks. Therefore, if MR is positive, the reliability of supplying power in the reconfigured network will improve and vice-versa, as compared to the base or original configuration.

3. Harmony Search Algorithm

The improvisation of musical harmony inspires the harmony search algorithm. HSA gives a set of solutions where the best solution is a near-optimum solution. The important feature of HSA is that it can independently consider each component variable in a single solution vector while it generates a new vector. This feature can accelerate the convergence rate of the HS algorithm by imposing constraints in the process of harmony improvisation (i.e., pitch adjustment, memory consideration, and random selection) for selecting a new decision variable. In HSA, discrete and continuous variables are managed together [3,4,35–38].

In the optimization process, HSA performs three functions described as:

a. Initialization of harmony memory
b. Improvisation of harmony memory
c. Updating the harmony memory

The harmony memory (HM) is a collection of possible solutions, depending upon the nature of the problem. Initially, HM is selected at random and/or based on prior information. The size of HM is operator-dependent, which further varies with the number of solution vectors and the complexity of the problem. Conversely, 'HM's improvisation can be achieved by selecting a new solution vector, at random, from either the initial solution space or the HM. The selection of a new solution vector from HM is decided based on the harmony memory considering rate (HMCR). Later, the pitch and bandwidth of such a selection is adjusted with a certain probability. Finally, the new harmony is evaluated, and the HM is updated based upon the audience response, i.e., improvement in the objective function corresponding to that selection.

A detailed explanation of HSA parameter selection is given in [3,4,35–38]. In Table 4, the effect of HSA parameters is summarized in the optimization function. Here, it can be noticed that the minimum power loss is obtained when HMCR is 0.85, PAR is 0.35, and HMS is 12 for the system under consideration. Therefore, with the change in HMCR, there is a significant change in the objective function.

Table 4. Results based on various HSA parameters for a 33-node radial distribution system.

Cases	HAS Parameter			Objective Function as Power Loss (kW)
	HMCR	PAR	HMS	
1	0.90	0.25	12	147.63
	0.70	0.25	12	143.44
	0.45	0.25	12	144.35
	0.35	0.25	12	155.73
2	0.85	0.35	12	139.55
	0.85	0.45	12	140.02
	0.85	0.55	12	139.97
	0.85	0.65	12	140.65

Table 4. *Cont.*

Cases	HAS Parameter			Objective Function as Power Loss (kW)
	HMCR	PAR	HMS	
	0.80	0.40	5	159.81
3	0.80	0.40	20	147.90
	0.80	0.40	25	162.68
	0.80	0.40	35	163.82

3.1. Harmony Improvisations

In HSA, the critical aspect is harmony improvisation. In harmony improvisation, there are three rules: namely, (a) random selection, (b) harmony memory consideration, and (c) pitch adjustment.

In the case of random selection, the new solution vector is selected from the global solution space with a probability of '1-HMCR'. Initially, with lower HMCR, the possibility of selection from global space is high. This is to explore the possible solution and to generate a solution vector in HM.

$$HMCR\,(t) = HMCR_{min} + \frac{(HMCR_{max} - HMCR_{min}) \times t}{T_{max}} \tag{27}$$

From (27), it can be observed that, with the increase in iteration, the HMCR increases, which, in turn, allows the higher probability of selection of a new solution vector from the HM. Further, the solution vector selected from HM has to be adjusted with the neighbor solution vector with PAR probability. The PAR increases with iteration and finally reaches '1', which means every solution vector needs to be pitch adjusted. The new vector, at this stage, is further modified with bandwidth. The PAR and bandwidth are defined using the following:

$$PAR\,(t) = PAR_{min} + \frac{(PAR_{max} - PAR_{min}) \times t}{T_{max}} \tag{28}$$

$$BW(t) = BW * e^{-\ln\left(\frac{BW_{min}}{BW_{max}}\right)\frac{t}{T_{max}}} \tag{29}$$

In (28) and (29), the PAR increases linearly, whereas BW decreases exponentially with an increase in iteration. This allows for the increase in probability for pitch adjustment with every increase in iteration, but it reduces the requirement of change in bandwidth at the same solution.

3.2. Solution Vector for PEBs

In the case of PEBs, the solution vector stored in the HM is limited to the tie-lines only. Therefore, in this case, the HM can be defined as

$$HSV^1 = \begin{bmatrix} TL_1^1 & TL_2^1 & TL_3^1 & TL_4^1 & TL_5^1 \dots\dots\dots \end{bmatrix} \tag{30}$$

In (30), each solution vector is defined corresponding to the respective tie-lines, and there may be any number of tie-lines in the sample system. Therefore, for a large network, it is required to generate a single solution vector in HSA.

3.3. Solution Vector for AEBs

In the case of AEBs, the solution vector stored in the HM is limited to twice the number of AEBs. Therefore, in this case, the HM can be defined as

$$HSV^1 = \begin{bmatrix} DG_1^1 & DG_2^1 & DG_3^1 \dots\dots ND_4^1 & ND_5^1 & ND_6^1 \dots\dots\dots \end{bmatrix} \tag{31}$$

In (31), $DG_1^1\ DG_2^1\ DG_3^1\ldots$ represents the solution vector, corresponding to the size of AEBs, and $ND_4^1\ ND_5^1\ ND_6^1\ldots$ represents the solution vector, corresponding to the locations of AEBs.

3.4. Solution Vector for PEBs and AEBs in Coordination

In the case of coordinated operation, the solution vector stored in the HM is the tie-lines, DG size, and its location at a particular node. Therefore, in this case, the HM can be defined as

$$HSV^1 = \begin{bmatrix} TL_1^1\ TL_2^1\ TL_3^1\ TL_4^1\ TL_5^1\ldots\ldots\ DG_6^1\ DG_7^1\ DG_8^1\ldots\ldots\ ND_9^1\ ND_{10}^1\ ND_{11}^1\ldots\ldots \end{bmatrix} \quad (32)$$

In (32), the solution vectors are represented, in coordination, for PEBs and AEBs, which were defined exclusively in (30) and (31), respectively.

4. Proposed Algorithm and Flowchart

Figure 2 shows the flow chart of the proposed algorithm. The steps involved in the proposed algorithm are described as follows:
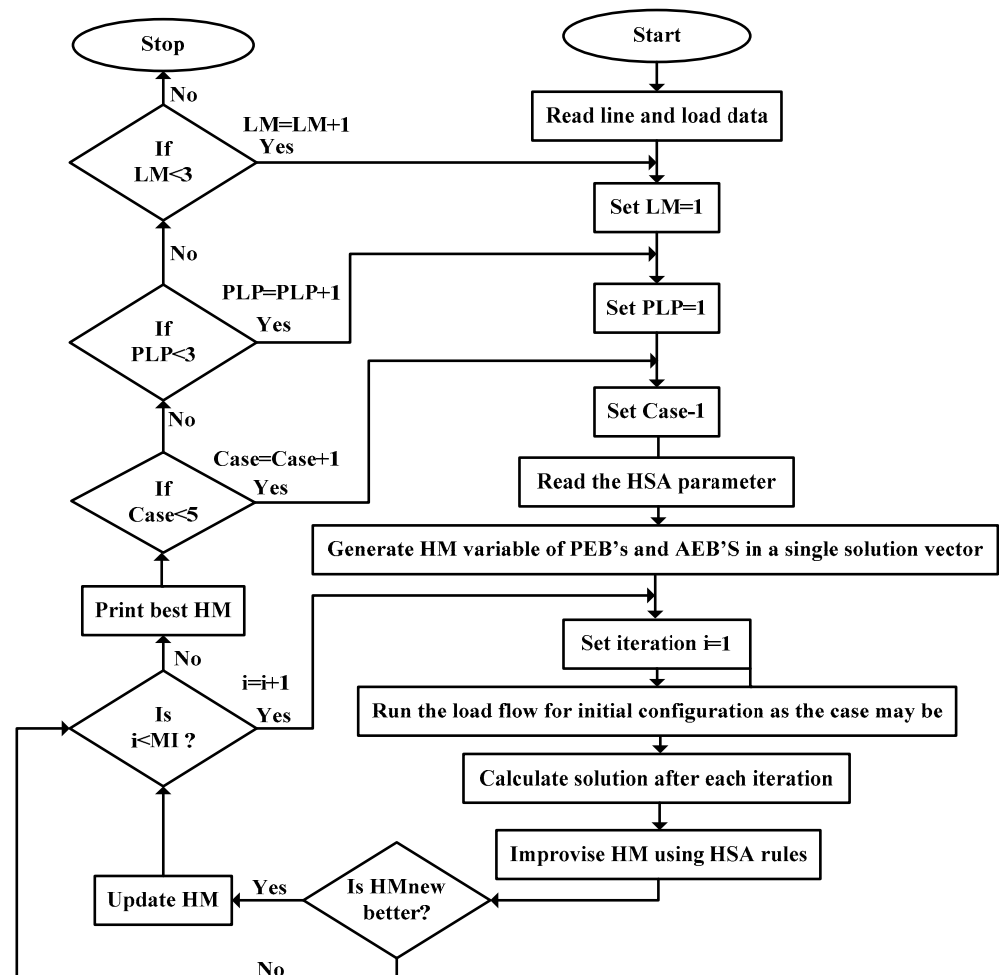

Figure 2. Flowchart of the proposed algorithm.

Step-1:　Read the line and load data.
Step-2:　Set LMs, PLPs, and cases of study
Step-3:　Run the load flow for initial configuration and save the result as reference.
Step-4:　Read the HSA parameters and generate HM, as per the solution vector described in Section 3.

Step-5: Set iteration counts = 1.
Step-6: Calculate the solution after each iteration and apply HSA rules for HM improvisation.
Step-7: If the new HM is better than the old, update HM, or else set counts = count + 1.
Step-8: In case-1, consider the following:

    a.   *run the load flow for LM-1, LM-2, and LM-3 under light, normal, and overloading scenario and find optimal configuration.*

    b.   *run the load flow for LM-1, LM-2, and LM-3 with 1DG, 2DG, and 3DG allocation in base configuration.*

    c.   *run the load flow for LM-1, LM-2, and LM-3 with 1DG, 2DG, and 3DG allocation in optimal configuration, which is obtained in (a).*

Step-9: In case-2, consider the following:

    a.   *run the load flow for LM-1 under normal loading scenario for 0%, 25%, and 50% SOC, with 1EV, 2EV, 3EV, and 4EVs as a load and find optimal configuration.*

    b.   *run the load flow individually for LM-2 and 3 under normal loading scenario for PLP-1, PLP-2, and PLP-3, with 1EV, 2EV, 3EV, and 4EVs as a load and find optimal configuration.*

Step-10: In case-3, consider the following;

    a.   *run the load flow for LM-1 under normal loading scenario for 0%, 25%, and 50% SOC, with 1EV, 2EV, 3EV, and 4EVs as a source and find optimal configuration.*

    b.   *run the load flow individually for LM-2 and 3 under normal loading scenario for PLP-1, PLP-2, and PLP-3, with 1EV, 2EV, 3EV, and 4EVs as a source and find optimal configuration.*

Step-11: In case-4, consider the following;

    a.   *run the load flow for LM-1 under normal loading scenario for 0%, 25%, and 50% SOC, with 1EV, 2EV, 3EV, and 4EVs as a load, at the most occurred location obtained in case 2 and 3, and find optimal configuration and DG allocation in coordination.*

    b.   *run the load flow individually for LM-2 and 3 under normal loading scenario for PLP-1, PLP-2, and PLP-3, with 1EV, 2EV, 3EV, and 4EVs as a load, at the most occurred location obtained in case 2 and 3, and find optimal configuration and DG allocation in coordination.*

Step-12: In case-5, consider the following;

    a.   *run the load flow for LM-1 under normal loading scenario for 0%, 25%, and 50% SOC, with 1EV, 2EV, 3EV, and 4EVs as a source, at the most occurred location obtained in case 2 and 3, and find optimal configuration and DG allocation in coordination.*

    b.   *run the load flow individually for LM-2 and 3 under normal loading scenario for PLP-1, PLP-2, and PLP-3, with 1EV, 2EV, 3EV, and 4EVs as a source, at the most occurred location obtained in case 2 and 3, and find optimal configuration and DG allocation in coordination.*

Step-13: Print the EEP under different LMs for different SOC, PLP, EVs, and DG allocations, as the case may be, of energy efficient configuration.

5. Test System, Assumptions and Cases of Study

5.1. Test System

In this work, a sample 33-node radial distribution system, as shown in Figure 3, is considered, and the proposed algorithm is demonstrated in the MATLAB environment. In this network, the branches or lines are divided into two parts, such as tie-lines and connected branches. The tie-lines are the branches made OFF from the network during operation, whereas the connected branches are the branches that remain in operation. Here, the base configuration is represented when tie-lines 33–37 are opened, and the other

configurations are obtained by changing the status of the switch from ON to OFF in other branches during optimization. The first node is the substation, and the voltage at that node is maintained as 1.0 pu.
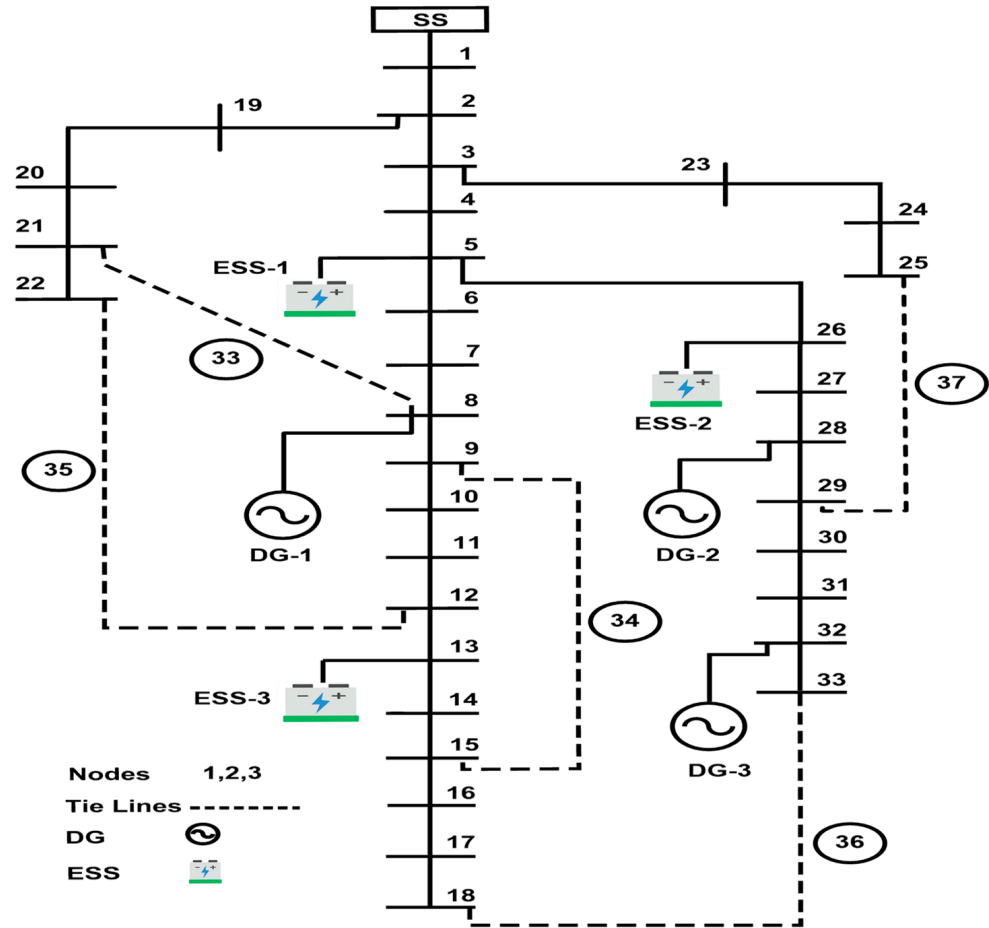
Figure 3. A sample 33-node radial distribution system.

5.2. Assumptions

The following are the assumptions while performing optimization in this work:

(a)   The substation can meet the power demand of the system
(b)   The maximum voltage at the substation is 1.0 pu.
(c)   The minimum and maximum voltage, at respective nodes, are 0.90 pu and 1.05 pu.
(d)   The maximum capacity of a single AEB is 1 MW at one location.
(e)   The switching loss is negligible.
(f)   The appropriate size of AEBs is available at the optimal location and can operate at their maximum capacity.

5.3. Energy Efficiency Analysis under Different Cases of Study

Table 5 shows the five different study cases for EEP analysis of the distribution system. However, these cases can be redefined as EEP evaluation when ESS works as a load or source. In the case-1, the EEP is analyzed without ESS. EEP realization of the network under consideration is presented in the following sections, from 6.1 to 6.5, exclusively, for all cases.

Table 5. The cases of study for EEP evaluation with PLP under different LMs.

Cases	Description	Remarks
Case-1	EEP evaluation of new configuration with PEBs and AEBs exclusively	This allows the EEP evaluation of reconfigured network and AEBs allocation in the original network and reconfigured network under different LMs **without ESS**.
Case-2	EEP evaluation with PEBs	This allows the change in a network topology for single/multi objectives and the EEP evaluation of the resulting configuration under different LMs **with ESS as a LOAD**.
Case-3	EEP evaluation with PEBs	This allows the change in a network topology for single/multi objectives and the EEP evaluation of the resulting configuration under different LMs **with ESS as a SOURCE**.
Case-4	EEP evaluation with PEBs and AEBs in coordination	This allows EEP evaluation in the coordination of PEBs and AEBs for energy-efficient operation under different LMs **with ESS as a LOAD**.
Case-5	EEP evaluation with PEBs and AEBs in coordination	This allows EEP evaluation in the coordination of PEBs and AEBs for energy-efficient operation under different LMs **with ESS as a SOURCE**.

6. Test Results and Discussions

6.1. Case-1: EEP Realization in Original and Reconfigured Topology (without ESS)

Table 6 shows the test result of the 33-node electrical system under different LMs for case-1. Here, the tie-lines in the original configuration are 33, 34, 35, 36, and 37, fixed, and the EEP is evaluated under light, normal, and overloading scenarios. Part-A of Table 6 shows that the optimal configuration obtained under the overloading scenario is different from the light and normal loading scenario in LM-1. However, in LM-2, the optimal configuration under light loading is different from the normal and overloading scenario. Conversely, in LM-3, the optimal configuration is the same under light, normal, and overloading scenarios.

The power loss under LM-2 and 3 is less than the LM-1 because the load profile in LM-1 is fixed, whereas it is voltage-dependent under LM-2 and 3, which draws less power if the voltage profile is lower than their nominal voltages at the load bus. As a result, the loadability margin has improved in the case of LM-2 and 3. Here, the %MR has been reduced over the various loading scenario, as shown in Part A of Table 6.

Similarly, Part B of Table 6 shows the EEP analysis of the original configuration when 1DG, 2DG, and 3DGs are placed at optimal locations under different LMs. All EEP parameters vary with the DG placement, but %MR in LM-1 is found unchanged. This is because the system's reliability depends upon the network configuration and loading patterns, which, in this case, are fixed. However, MR has increased in LM-2 and 3 with DG placements. Part-C of Table 6 shows the EEP analysis of reconfigured networks, obtained in Part-A, with optimal 1DG, 2DG, and 3DG placement. Here, it can be noticed that the power losses have reduced, and MR has increased under all LMs. When DGs are placed in the optimal configuration, obtained in Part-A, the reduced DG size can significantly improve the EEP compared to the original configuration's DG allocation.

6.2. Case-2: EEP Realization with PEBs (ESS Works as a Load)

Table 7 shows the test result of the 33-node electrical system under different LMs for case-2. The original configuration, with tie lines as 33, 34, 35, 36, and 37, is fixed, and the EEP is evaluated under different LMs. In LM-1, three different cases are developed where PCF is taken as 0.0, 0.25, and 0.50 when ESS works as a load. The EEP of an electrical system is also evaluated for single, two, three, and four ESS.

Table 6. EEP for Case-1 (reconfiguration and DG allocation exclusively).

	A. EEP analysis of reconfigured network								
	EEP evaluation under LM-1			EEP evaluation under LM-2			EEP evaluation under LM-3		
Loading scenario	Light	Normal	Over	Light	Normal	Over	Light	Normal	Over
Optimal Conf	7, 14, 9, 32, 37	7, 14, 9, 32, 37	7, 14, 9, 32, 28	7, 14, 9, 32, 28	7, 14, 9, 32, 37	7, 14, 9, 32, 37	7, 14, 9, 32, 37	7, 14, 9, 32, 37	7, 14, 9, 32, 37
V_{min}	0.9508	0.9378	0.9287	0.9553	0.9410	0.9292	0.9512	0.9384	0.9254
$F_{si,min}$	18.53	14.73	12.20	19.11	15.32	12.80	18.63	14.84	12.31
P_L, (kW)	87.59	139.55	205.62	81.86	127.47	183.59	86.43	137.20	200.80
%MR	1.2812	1.2812	2.3501	2.2355	1.1569	1.1302	1.2622	1.2566	1.2505
	B. EEP analysis of original network with DG allocations								
	EEP evaluation under LM-1			EEP evaluation under LM-2			EEP evaluation under LM-3		
AEBs scenario	1DG	2DG	3DG	1DG	2DG	3DG	1DG	2DG	3DG
Original Conf	33, 34, 35, 36, 37	33, 34, 35, 36, 37	33, 34, 35, 36, 37	33, 34, 35, 36, 37	33, 34, 35, 36, 37	33, 34, 35, 36, 37	33, 34, 35, 36, 37	33, 34, 35, 36, 37	33, 34, 35, 36, 37
DG size (Node)	1975 (7)	1078 (11) 1032 (30)	945 (30) 796 (25) 716 (14)	1976 (7)	1304 (30) 780 (13)	882 (10) 943 (30) 868 (24)	2190 (7)	1138 (29) 779 (14)	765 (25) 726 (14) 952 (30)
V_{min}	0.9450	0.9673	0.9629	0.9472	0.9708	0.9620	0.9515	0.9659	0.9658
$F_{si,min}$	22.13	29.29	25.26	22.83	29.36	27.03	23.35	29.08	26.87
P_L, (kW)	108.31	86.24	73.49	102.50	85.51	72.87	97.88	81.11	68.50
%MR	–	–	–	−0.0420	−0.0302	−0.0178	−0.0765	−0.1250	−0.1327
	C. EEP analysis of reconfigured network with DG allocations								
	EEP evaluation under LM-1			EEP evaluation under LM-2			EEP evaluation under LM-3		
AEBs scenario	1DG	2DG	3DG	1DG	2DG	3DG	1DG	2DG	3DG
Optimal Conf	7, 14, 9, 32, 37	7, 14, 9, 32, 37	7, 14, 9, 32, 28	7, 14, 9, 32, 28	7, 14, 9, 32, 37	7, 14, 9, 32, 37	7, 14, 9, 32, 37	7, 14, 9, 32, 37	7, 14, 9, 32, 37
DG size (Node)	1030 (30)	881 (9) 1080 (29)	944 (30) 963 (8) 855 (24)	1571 (25)	1693 (25) 865 (8)	861 (9) 792 (30) 879 (24)	1570 (25)	907 (8) 1372 (25)	903 (24) 759 (30) 811 (8)
V_{min}	0.9478	0.9707	0.9732	0.9489	0.9725	0.9732	0.9507	0.9694	0.9720
$F_{si,min}$	14.75	30.08	32.53	14.94	30.13	29.64	15.42	32.24	29.43
P_L, (kW)	98.19	73.54	59.46	85.70	61.86	59.28	81.58	60.06	56.45
%MR	−0.8123	−0.8123	−0.8123	−0.7195	−0.7468	−0.7103	−0.7716	−0.8404	−0.8292

Table 7. EEP for Case-2 (when ESS works as a load).

A. EEP evaluation under LM-1

With	With 1EV Station			With 2EV Station			With 3EV Station			With 4EV Station		
SOC	0%	25%	50%	0%	25%	50%	0%	25%	50%	0%	25%	50%
Optimal EVS (Location)	24	2	5	5, 2	27, 2	10, 19	23, 5, 2	30, 6, 2	24, 2, 19	18, 5, 19, 2	19, 4, 28, 13	13, 23, 2, 28
Optimal Conf	7, 14, 10, 32, 37	7, 13, 9, 36, 28	7, 14, 9, 32, 37	7, 14, 10, 32, 28	7, 13, 9, 32, 28	7, 14, 9, 32, 28	6, 14, 10, 36, 37	7, 14, 10, 36,28	7, 14, 9, 36, 37	7, 34, 10, 17, 28	7, 14, 10, 36, 28	7, 34, 10, 36, 28
V_{min}	0.9370	0.9377	0.9369	0.9403	0.9402	0.9411	0.9336	0.9327	0.9330	0.9226	0.9354	0.9360
$F_{si,min}$	14.72	15.58	14.73	14.71	14.68	13.83	13.19	15.26	15.62	14.24	13.80	14.54
P_L, (kW)	148.10	145.29	143.01	147.77	149.81	147.01	162.97	164.78	148.31	183.94	174.35	163.09
%MR	−1.0526	−0.6973	−0.8123	−0.9409	−0.7283	−0.6982	−1.5227	−0.9105	−0.7816	−0.5477	−0.9105	−0.7326

B. EEP evaluation under LM-2

With	With 1EV Station			With 2EV Station			With 3EV Station			With 4EV Station		
SOC (60–100%)	PLP = 1	PLP = 2	PLP = 3	PLP = 1	PLP = 2	PLP = 3	PLP = 1	PLP = 2	PLP = 3	PLP = 1	PLP = 2	PLP = 3
Optimal EVS (Location)	18	33	32	18, 32	32, 15	15, 31	10, 33, 15	31, 15, 18	16, 15, 18	15, 30, 32, 31	16, 32, 18, 14	32, 30, 18, 14
Optimal Conf	7, 14, 9, 32, 37	7, 14, 10, 32, 28	7, 14, 9, 31, 28	7, 13, 9, 31, 28	7, 14, 9, 31, 37	7, 14, 9, 30, 37	6, 14, 9, 31, 37	6, 14, 9, 31, 37	7, 13, 10, 30, 37	7, 34, 10, 31, 27	7, 14, 10, 30, 37	7, 13, 9, 30, 37
V_{min}	0.9396	0.9442	0.9460	0.9526	0.9524	0.9446	0.9559	0.9500	0.9440	0.9512	0.9601	0.9553
$F_{si,min}$	16.48	17.05	17.35	17.35	16.92	15.82	17.07	17.16	17.74	17.41	20.51	18.96
P_L, (kW)	124.17	118.33	104.40	103.07	100.24	92.91	87.19	91.43	87.19	82.25	80.21	74.88
%MR	−0.8491	−1.0015	−0.7938	−0.7784	−0.9003	−0.6252	−1.4383	−1.4025	−0.9168	−0.7571	−0.8689	−0.6699

C. EEP evaluation under LM-3

With	With 1EV Station			With 2EV Station			With 3EV Station			With 4EV Station		
SOC (60–100%)	PLP = 1	PLP = 2	PLP = 3	PLP = 1	PLP = 2	PLP = 3	PLP = 1	PLP = 2	PLP = 3	PLP = 1	PLP = 2	PLP = 3
Optimal EVS (Location)	31	16	16	30, 32	29, 18	15, 32	18, 29, 15	8, 31, 33	32, 30, 14	30, 29, 17, 31	32, 31, 33, 25	32, 30, 16, 18
Optimal Conf	7, 14, 9, 36, 37	7, 14, 9, 31, 37	7, 14, 9, 31, 37	7, 14, 9, 31, 28	7, 14, 10, 31, 37	7, 14, 10, 31, 28	7, 14, 9, 31, 37	7, 14, 10, 31, 28	7, 13, 9, 31, 37	7, 14, 9, 30, 28	7, 14, 10, 31, 28	6, 13, 9, 31, 37
V_{min}	0.9441	0.9388	0.9337	0.9437	0.9446	0.9507	0.9542	0.9568	0.9469	0.9479	0.9639	0.9528
$F_{si,min}$	16.27	14.64	13.75	14.82	15.27	16.36	17.61	18.28	17.27	15.86	18.27	16.06
P_L, (kW)	116.19	114.33	124.65	103.44	102.09	105.97	85.70	83.18	89.70	80.11	74.13	84.53
%MR	−0.8572	−0.8825	−0.8515	−0.7700	−1.1233	−0.9918	−0.9064	−1.0288	−0.9881	−0.4787	−1.0305	−1.3883

The location of ESS, in these cases, is found to be different under different LMs, as shown in Table 7. The 0% SOC means ESS is wholly discharged and acts as a load of its total capacity, similar to 25% and 50%. Since ESS works as a load, the overall loading patterns of the system will increase, and as a result, the power loss may increase under different LMs. Here, the optimization is performed for ESS locations under different LMs. Part A of Table 7 shows the optimal location of ESS when it works as a load, found at node numbers 24, 2, and 5 in LM-1, with SOC as 0, 25, and 50%, respectively.

The optimal location of ESS varies with LMs and is found at 18, 33, and 32 in LM-2, as well as 31, 16, and 16 in LM-3 for one EV station, as shown in Part B and C of Table 7. Here, it can also be noticed that the optimum location of ESS and the resulting configurations are found to be different for 2EV, 3EV, and 4EVs under different LMs. However, the MR is increased compared to the original configuration in these configurations.

Here, it can also be observed that the optimal configuration, under different loading patterns, is found to be different. The variation in the resulting configuration and the ESS location may further alter the %MR for 1EV, 2EV, 3EV, and 4EVs. Though ESS works as a load, the power loss in the resulting optimal configuration is slightly greater compared to the optimal configurations obtained in case-1, as shown in Table 6.

6.3. Case-3: EEP Realization with PEBs (ESS Works as a Source)

Table 8 shows the test result for EEP realization with PEBs for case-3 when ESS works as a source. In this case, the EVs location was found to be different in comparison with the previous case. Additionally, the optimal configuration and other EEP parameters vary significantly. The optimal configuration, with tie-lines 7, 9, 14, 23, and 27, is obtained for LM-1 with 1EV under 0% SOC. Similarly, the optimal configuration is the same for 25% and 50% SOC, whereas the other EEP parameters are different.

The optimal configuration under the same EVs may be different. It can be noticed that the optimal configuration with 2EV, 3EV, and 4EVs under 50% SOC are found to be 7, 9, 14, 32, 37, 7, 9, 14, 32, 28, as well as 7, 9, 14, 32, and 37. The difference in optimal configuration can also be observed under 0% and 25% SOC. EVs work as a source to alter the load profile and relieve the demand at that node. Here, the system losses have been reduced, and the loadability margin has improved because of the improvement in voltage profile. From the results, it can be observed that the margin of reliability has also been improved.

However, under LM-1, the power loss across 1EV, 2EV 3EV, and 4EVs varies slightly, whereas the reduction in loss, in the case of LM-2 and LM-3, is found to be very significant. These losses are 135.47, 134.25, 132.47, and 126.48, in the case on LM-2, and 126.26, 123.84, 121.60, and 119.77 kW in the case of LM-3, respectively. The reduction in power loss and improvement in the voltage profile further help improve the loadability margin and MR. For example, with 1EV, the f_{si} for 0% SOC in LM-1 is 14.74, whereas, for LM-2 and LM-3, they are 15.05 and 15.46, respectively.

6.4. Case-4: EEP Realization with PEBs and AEBs in Coordination (ESS Works as a Load)

Unlike the above two cases, case-4 considers the PEBs and AEBs in coordination, where optimization is performed when ESS works as a load. The coordinated operation of PEBs and AEBs allows for finding the optimal configuration and DGs allocation with 1EV, 2EV, 3EV, and 4EVs under different loading patterns, as shown in Table 9. Part A of Table 9 offers the EEP evaluation under LM-1. Here, three different cases are considered, such as 0%, 25%, and 50% SOC in the case of LM-1, as well as PLP-1, PLP-2, and PLP-3 in the case of LM-2 and LM-3. The optimal location of EVs is decided based on their locations in case-2 and 3, as shown in Tables 7 and 8. Here, the most occurred site of EVs is identified, and later, with their fixed location, the optimization is performed for coordinated operation. In LM-1, with 1EV, the most occurred site is at node 18, and for 2EVs, it is at node 2 and 19. A similar check is performed for 3EVs and 4EVs across all cases under LM-2 and LM-3.

Table 8. EEP for Case-3 (when ESS works as a source).

	With 1EV Station			With 2EV Station			With 3EV Station			With 4EV Station		
A. EEP evaluation under LM-1												
With SOC	0%	25%	50%	0%	25%	50%	0%	25%	50%	0%	25%	50%
Optimal EVS(Location)	31	32	33	31, 17	9, 18	29, 32	8, 18, 31	16, 30, 31	17, 31, 32	16, 24, 31, 32	8, 15, 27, 33	17, 18, 28, 33
Optimal Conf	7, 9, 14, 23, 37	7, 9, 14, 23, 37	7, 9, 14, 23, 37	7, 9, 14, 23, 37	7, 9, 14, 23, 37	7, 9, 14, 32, 37	7, 14, 10, 32, 37	7, 9, 14, 32, 37	7, 9, 14, 28, 32	7, 9, 14, 32, 37	7, 9, 14, 32, 37	7, 9, 14, 32, 37
V_{min}	0.9386	0.9386	0.9378	0.9387	0.9378	0.9390	0.9391	0.9398	0.9429	0.9405	0.9384	0.9385
$F_{si,min}$	14.73	14.73	14.89	15.04	15.21	14.77	15.33	15.02	15.02	14.98	15.46	15.40
P_L, (kW)	137.87	138.03	138.24	135.55	136.19	136.97	133.44	133.24	133.97	131.70	133.11	133.02
%MR	−0.8123	−0.8123	−0.8123	−0.8123	−0.8123	−0.8123	−1.0526	−0.8123	−0.6982	−0.8123	−0.8123	−0.8123
B. EEP evaluation under LM-2												
With SOC (60–100%)	PLP = 1	PLP = 2	PLP = 3	PLP = 1	PLP = 2	PLP = 3	PLP = 1	PLP = 2	PLP = 3	PLP = 1	PLP = 2	PLP = 3
Optimal EVS (Location)	12	27	9	15, 31	8, 33	9, 32	15, 17, 32	15, 16, 33	14, 30, 31	8, 10, 29, 32	7, 17, 32, 15	14, 12, 15, 32
Optimal Conf	7, 9, 14, 32, 37	7, 9, 14, 32, 37	7, 9, 14, 32, 37	7, 9, 14, 32, 37	7, 9, 14, 28, 32	7, 9, 14, 32, 37	7, 9, 14, 32, 37	7, 9, 14, 28, 32	7, 10, 14, 32, 37	7, 9, 14, 32, 37	7, 14, 10, 32, 37	7, 9, 14, 28, 32
V_{min}	0.9386	0.9413	0.9433	0.9394	0.9441	0.9429	0.9396	0.9442	0.9454	0.9416	0.9428	0.9470
$F_{si,min}$	15.06	15.32	15.91	14.99	15.76	15.75	15.20	16.16	15.95	15.48	15.72	16.53
P_L, (kW)	135.47	126.77	118.73	134.25	125.25	120.93	132.47	122.71	115.13	126.48	121.93	114.41
%MR	−0.8274	−0.8707	−0.9091	−0.8226	−0.7482	−0.8912	−0.8217	−0.7523	−1.1480	−0.8474	−1.1124	−0.7822
C. EEP evaluation under LM-3												
With SOC (60–100%)	PLP = 1	PLP = 2	PLP = 3	PLP = 1	PLP = 2	PLP = 3	PLP = 1	PLP = 2	PLP = 3	PLP = 1	PLP = 2	PLP = 3
Optimal EVS(Location)	18	32	33	18,30	24,31	15,31	12,28,29	18,30, 33	14,31,33	16,17, 30, 33	30,31, 27,18	18,31, 32,33
Optimal Conf	7, 9, 14, 32, 37	7, 9, 14, 32, 37	7, 9, 14, 32, 37	7, 9, 14, 32, 37	7, 9, 14, 28, 32	7, 9, 14, 28, 32	7, 9, 14, 32, 37	7, 14, 10, 32, 37	7, 9, 14, 32, 37	7, 9, 14, 32, 37	7, 9, 14, 32, 37	7, 14, 10, 32, 37
V_{min}	0.9410	0.9413	0.9393	0.9417	0.9449	0.9427	0.9431	0.9415	0.9397	0.9424	0.9433	0.9405
$F_{si,min}$	15.46	15.26	15.19	15.64	15.26	15.13	15.54	15.72	15.34	16.06	15.46	15.54
P_L, (kW)	126.65	127.53	132.50	123.84	126.60	133.29	121.60	124.39	131.37	119.77	121.85	128.37
%MR	−0.8722	−0.8660	−0.8409	−0.8781	−0.7413	−0.7141	−0.8767	−1.1081	−0.8270	−0.8865	−0.8723	−1.0800

Table 9. EEP for Case-4 (ESS works as a load).

A. EEP evaluation under LM-1

With SOC	With 1EV Station			With 2EV Station			With 3EV Station			With 4EV Station		
	0%	25%	50%	0%	25%	50%	0%	25%	50%	0%	25%	50%
Optimal Conf	7, 14, 10, 28, 31	9, 28, 31, 33, 34	7, 9, 13, 28, 31	9, 26, 30, 33, 34	7, 10, 28, 30, 34	7, 9, 13, 28, 36	7, 9, 14, 28, 30	7, 12, 28, 31, 35	7, 13, 28, 32, 35	6, 9, 13, 27, 30	10, 28, 31, 33, 34	10, 14, 28, 31, 33
Optimal EVS (Location)	18	18	18	2, 19	2, 19	2, 19	2, 19, 23	2, 19, 23	2, 19, 23	2, 19, 23, 30	2, 19, 23, 30	2, 19, 23, 30
DG	691 (33) 428 (12) 877 (25)	933 (15) 885 (7) 990 (30)	952 (29) 548 (8) 615 (17)	890 (17) 568 (7) 923 (25)	820 (21) 693 (17) 932 (25)	773 (32) 836 (25) 709 (15)	612 (13) 795 (33) 867 (25)	696 (18) 996 (29) 568 (8)	662 (29) 977 (25) 775 (16)	778 (18) 975 (29) 797 (7)	755 (33) 954 (25) 721 (26)	837 (30) 688 (15) 784 (7)
V_{min}	0.9684	0.9656	0.9710	0.9599	0.9553	0.9785	0.9732	0.9721	0.9728	0.9681	0.9703	0.9712
$F_{si,min}$	27.16	31.73	28.19	26.07	24.58	28.47	28.04	30.81	27.31	24.46	30.78	28.96
P_L, (kW)	59.71	55.39	59.04	57.86	58.97	59.77	57.64	59.87	61.60	59.53	56.42	61.55
%MR	−0.9553	0.0017	−0.7455	0.2208	−0.4815	−0.6964	−0.4128	−0.4004	−0.6657	−0.9202	−0.2524	−0.4389

B. EEP evaluation under LM-2

With SOC (60–100%)	With 1EV Station			With 2EV Station			With 3EV Station			With 4EV Station		
	PLP = 1	PLP = 2	PLP = 3	PLP = 1	PLP = 2	PLP = 3	PLP = 1	PLP = 2	PLP = 3	PLP = 1	PLP = 2	PLP = 3
Optimal Conf	7, 10, 13, 28, 32	7, 9, 28, 32, 34	9, 14, 28, 30, 33	10, 14, 27, 30, 33	6, 13, 16, 35,37	10, 14, 28, 30, 33	9, 14, 28, 30, 33	9, 28, 31, 33, 34	7, 10, 13, 28, 31	7, 9, 13, 32, 37	10, 13, 28, 30, 33	6, 9, 26, 31, 34
Optimal EVS (Location)	18	18	18	2, 19	2, 19	2, 19	2, 19, 23	2, 19, 23	2, 19, 23	2, 19, 23, 30	2, 19, 23, 30	2, 19, 23, 30
DG	785 (31) 746 (14) 996 (24)	662 (31) 816 (24) 826 (14)	977 (25) 699 (17) 930 (7)	670 (25) 655 (33) 931 (8)	963 (30) 996 (8) 955 (24)	610 (25) 921 (7) 626 (32)	946 (7) 812 (29) 753 (33)	890 (4) 914 (30) 787 (17)	683 (24) 771 (16) 693 (30)	863 (25) 852 (30) 691 (15)	625 (18) 925 (29) 601 (8)	947 (29) 612 (8) 793 (15)
V_{min}	0.9757	0.9745	0.9739	0.9714	0.9660	0.9728	0.9728	0.9722	9632	0.9699	0.9631	0.9633
$F_{si,min}$	26.71	29.64	29.46	29.58	35.42	31.21	28.58	30.79	22.60	25.72	34.77	28.27
P_L, (kW)	58.39	56.11	53.37	58.68	57.02	53.96	57.57	56.57	55.16	58.09	57.52	55.30
%MR	−0.9806	−0.6383	−0.0501	−0.1342	−1.0598	−0.3125	0.1254	−0.1120	−1.1570	−0.8885	−0.2734	−1.3336

C. EEP evaluation under LM-3

With SOC (60–100%)	With 1EV Station			With 2EV Station			With 3EV Station			With 4EV Station		
	PLP = 1	PLP = 2	PLP = 3	PLP = 1	PLP = 2	PLP = 3	PLP = 1	PLP = 2	PLP = 3	PLP = 1	PLP = 2	PLP = 3
Optimal Conf	6, 10, 13, 28, 30	9, 27, 30, 33, 34	7, 13, 26, 32, 35	7, 9, 14, 28,30	7, 9, 13, 27,30	7, 9, 13, 28, 32	7,8,28, 32, 34	7, 9, 13, 28, 32	7, 10, 14, 28,30	7,9,12, 28, 31	10, 27, 30, 33, 34	7, 12, 28, 32, 35
Optimal EVS (Location)	18	18	18	2, 19	2, 19	2, 19	2, 19, 23	2, 19, 23	2, 19, 23	2, 19, 23, 30	2, 19, 23, 30	2, 19, 23, 30
DG	632 (9) 947 (25) 610 (33)	957 (25) 920 (8) 741 (18)	831 (29) 856 (15) 860 (25)	667 (11) 827 (30) 641 (31)	735 (12) 797 (32) 984 (25)	666 (25) 733 (15) 979 (29)	664 (14) 922 (24) 750 (29)	745 (9) 848 (24) 807 (29)	934 (29) 942 (8) 482 (31)	985 (25) 613 (23) 834 (18)	984 (18) 749 (25) 889 (7)	935 (30) 886 (24) 883 (15)
V_{min}	0.9614	0.9579	0.9741	0.9680	0.9717	0.9760	0.9692	0.9687	0.9701	0.9702	0.9732	0.9760
$F_{si,min}$	21.05	24.21	30.09	27.42	25.60	26.51	25.80	27.51	28.95	22.80	31.06	30.57
P_L (kW)	55.32	54.99	58.58	57.33	56.81	59.58	56.29	57.65	57.23	57.56	54.64	56.64
%MR	−1.3101	0.2732	−0.8319	−0.5304	−0.5192	−0.7529	−0.6434	−0.8319	−0.7244	−0.5743	−0.0033	−0.4092

As shown in Part-A of Table 9, the optimal configuration with 1EV for 0% SOC is 7, 14, 10, 28, 31, for 25% SOC is 9, 28, 31, 33, 34, and for 50% SOC is 7, 9, 13, 28, 31. The location of EVs is the same across PLPs, whereas the optimal configuration is found to be different. The DG allocations vary differently, and they are 632 kW at 9th node, 947 kW at node 25, and 610 kW at node 33 for PLP-1, whereas, for PLP-2, the DGs are 957 kW at node 25, 920 kW at node 8, and 741 kW at node 18 in the case of LM-3, as shown in Part C of Table 9. In these cases, the reduction in power loss is found significantly improved compared to the original configuration, as shown in Table 6. Here, it can also be observed that improvement in node voltage increases the loading profile at respective nodes with the DG placement. Compared to the original configuration, some configurations can reduce the MR.

6.5. Case-5: EEP Realization with PEBs and AEBs in Coordination (ESS Works as Source)

Table 10 shows the EEP realization of the sample distribution system, with PEBs and AEBs in coordination, when ESS works as a source. Here, three different cases are also considered for EEP evaluation.

Part-A of Table 10 shows the EEP analysis with LM-1 under different cases of SOC. Similar to case-4, the most occurred location of EVs is identified, and later, with their fixed location, the optimization is performed for a coordinated operation. In LM-1, with 1EV, the most occurred location is at node 32, and for 2EVs, it is at node 18 and 32. A similar check is performed for 3EVs and 4EVs across all cases under LM-2 and LM-3.

As shown in Part-A of Table 10, the optimal configuration with 1EV for 0% SOC is 10, 27, 30, 33, 34, for 25% SOC is 7, 8, 12, 26, 31, and for 50% SOC is 7, 10, 14, 28, and 30. In these configurations, the EEP is found to be different.

6.6. Comparative Analysis of EEP with PEBs and AEBs across All the Cases

In a smart city environment, the EEP varies differently in the presence of ESS. In recent years, the use of electric vehicles has increased manifold, which demands smart operation, control, and monitoring. The smart process does require realizing the EEP from different perspectives. Sections 6.1–6.5 present the EEP realization in five separate cases. As described in Section 5, ESS is involved in all the cases except case-1. Therefore, case-1 represents the generalized EEP under different loading scenarios, whereas, in other cases, the ESS either works as a load or source depending upon their charging or discharging states. Table 6 presents the EEP of distribution with three loading scenarios: light, normal, and overload. With LM-1, under normal loading, as shown in Part-A of Table 6, the optimal configuration is 7, 9, 14, 32, 37, whereas, for overloading, it is 7, 9, 14, 28, 32. It shows that the optimal configuration is different when loading patterns change, even in the absence of ESS.

Conversely, integrating ESS with the existing system, as a load or source, can significantly affect the loading patterns. Therefore, EEP of the distribution network needs to be realized at the planning stage to identify the most economical location may not be optimal for EV stations. This aspect has been realized, in this work, through four different cases where EEP is evaluated with PEBs and AEBs when ESS works exclusively as a load or source. However, case-2 and 3 present the EEP with PEBs and ESS. In these cases, the optimal configuration under LM-1 (with 50% SOC) is found to be 7, 9, 14, 32, 37 and 7, 9, 14, 23, 37, respectively. Here, it can be noticed that, in case-2, the ESS works as a load, whereas case-3 works as a source. On comparing case-2 and 3 with case-1, the EEP is found to vary differently. The third aspect of the proposed approach, i.e., case-4 and 5, is EEP realization with PEBs, AEBs, and ESS in coordination. EEP, in cases 2 and 3, varies with ESS as a load or source; therefore, in cases 4 and 5, the coordinated operation is realized accordingly. In these cases, the optimal location of DGs and the ESS differ. Here, some locations are found repeatedly across different LMs in case-4 and 5. From across four cases, the optimal location of ESS is identified: node 18 for 1EV, nodes 2 and 19 for 2EVs, nodes 2, 19, and 23 for 3EVs, and nodes 2, 19, 23, and 30 for 4EVs when ESS works as a load. On the other hand, the optimal location of EV stations when ESS works as a source is node 32 for 1EV, nodes 18 and 32 for 2EVs, nodes 17, 18, and 32 for 3EVs, and nodes 17, 18, 30, and 32 for 4EVs.

Table 10. EEP for Case-5 (ESS works as a source).

A. EEP evaluation under LM-1											
With SOC	**With 1EV Station**			**With 2EV Station**			**With 3EV Station**			**With 4EV Station**		
	0%	25%	50%	0%	25%	50%	0%	25%	50%	0%	25%	50%
Optimal Conf	10, 27, 30, 33, 34	7, 8, 12, 26, 31	7, 10, 14, 28, 30	10, 28, 31, 33, 34	10, 13, 28, 30, 33	6, 9, 13, 28, 30	10, 14, 28, 30, 33	10, 14, 28, 30, 33	6, 9, 12, 17, 28	10, 27, 31, 33, 34	10, 13, 26, 30, 33	7, 12, 10, 27, 32
Optimal EVS(Location)	32	32	32	18, 32	18, 32	18, 32	18, 32, 17	18, 32, 17	18, 32, 17	18, 32, 17, 30	18, 32, 17, 30	18, 32, 17, 30
DG	904 (18) 767 (7) 833 (29)	857 (16) 838 (24) 942 (29)	964 (25) 549 (13) 883 (33)	630 (15) 734 (25) 908 (7)	782 (33) 834 (7) 889 (25)	766 (18) 925 (29) 832 (8)	816 (7) 650 (32) 902 (30)	915 (26) 808 (25) 764 (31)	574 (25) 862 (9) 755 (32)	800 (26) 824 (16) 713 (29)	842 (8) 731 (33) 944 (25)	906 (29) 804 (15) 882 (24)
V_{min}	0.9692	0.9593	0.9765	0.9582	0.9752	0.9703	0.9754	0.9754	0.9721	0.9687	0.9748	0.9728
$F_{si,min}$	29.01	22.50	28.78	27.84	34.39	25.27	31.39	31.39	27.97	26.74	32.45	29.58
P_L, (kW)	54.94	59.78	56.97	58.66	55.49	57.58	56.77	57.69	61.11	58.56	57.07	56.25
%MR	−0.1137	−0.5635	−0.6639	−0.2555	−0.1613	−0.9775	−0.1322	−0.1320	−0.8058	−0.2126	−0.2690	−0.6587
B. EEP evaluation under LM-2											
With SOC (60–100%)	**With 1EV Station**			**With 2EV Station**			**With 3EV Station**			**With 4EV Station**		
	PLP = 1	PLP = 2	PLP = 3	PLP = 1	PLP = 2	PLP = 3	PLP = 1	PLP = 2	PLP = 3	PLP = 1	PLP = 2	PLP = 3
Optimal Conf	11, 14, 28, 30, 33	7, 10, 14, 28, 30	7, 12, 10, 32, 37	7, 8, 32, 34, 37	7, 13, 28, 30, 35	9, 13, 26, 30, 33	7, 9, 14, 28, 30	9, 26, 31, 33, 34	6, 9, 13, 31, 37	7, 9, 14, 28, 30	7, 9, 13, 28, 30	7, 10, 27, 31, 34
Optimal EVS (Location)	32	32	32	18, 32	18, 32	18, 32	18, 32, 17	18, 32, 17	18, 32, 17	18, 32, 17, 30	18, 32, 17, 30	18, 32, 17, 30
DG	880 (25) 877 (5) 790 (32)	594 (32) 831 (22) 985 (25)	790 (30) 856 (15) 755 (25)	806 (25) 874 (12) 965 (28)	628 (33) 886 (25) 736 (8)	830 (29) 561 (18) 812 (6)	858 (18) 756 (7) 967 (25)	966 (30) 557 (8) 871 (15)	531 (29) 876 (15) 810 (24)	915 (25) 556 (32) 437 (22)	613 (31) 966 (24) 778 (20)	472 (18) 555 (8) 950 (29)
V_{min}	0.9755	0.9668	0.9714	0.9662	0.9659	0.9664	0.9672	0.9706	0.9625	0.9603	0.9643	0.9664
$F_{si,min}$	34.26	24.37	31.39	30.87	28.84	32.12	19.94	29.57	20.58	21.88	22.95	29.62
P_L, (kW)	57.81	53.02	53.14	60.50	55.49	54.80	57.38	55.35	55.63	58.36	57.58	53.67
%MR	−0.0852	−0.7734	−1.0477	−0.6443	−0.4915	−0.1927	−0.4482	−0.2100	−1.5506	−0.4392	−0.5456	−0.9368
C. EEP evaluation under LM-3											
With SOC (60–100%)	**With 1EV Station**			**With 2EV Station**			**With 3EV Station**			**With 4EV Station**		
	PLP = 1	PLP = 2	PLP = 3	PLP = 1	PLP = 2	PLP = 3	PLP = 1	PLP = 2	PLP = 3	PLP = 1	PLP = 2	PLP = 3
Optimal Conf	10, 28, 31, 33, 34	7, 8, 32, 34, 37	10, 14, 28, 31, 33	7, 11, 14, 31, 37	7, 8, 28, 32, 34	7, 9, 12, 27, 30	7, 12, 27, 31, 35	10, 13, 28, 31, 33	7, 9, 25, 32, 34	7, 9, 26, 30, 34	6, 8, 13, 27, 31	6, 9, 12, 16, 28
Optimal EVS (Location)	32	32	32	18, 32	18.32	18, 32	18, 32, 17	18, 32, 17	18, 32, 17	18, 32, 17, 30	18, 32, 17, 30	18, 32, 17, 30
DG	878 (16) 979 (6) 714 (31)	848 (25) 678 (12) 889 (30)	610 (26) 653 (18) 946 (29)	854 (16) 834 (24) 941 (29)	793 (15) 663 (31) 820 (25)	851 (25) 839 (17) 673 (22)	908 (24) 866 (15) 918 (30)	912 (25) 815 (8) 607 (33)	680 (15) 813 (24) 977 (29)	807 (33) 648 (8) 914 (29)	690 (8) 670 (17) 870 (25)	843 (24) 871 (32) 893 (8)
V_{min}	0.9738	0.9610	0.9740	0.9724	0.9788	0.9644	0.9605	0.9712	0.9708	0.9719	0.9672	0.9748
$F_{si,min}$	28.55	26.02	31.41	23.79	29.41	24.11	24.89	31.48	26.77	28.59	27.79	31.51
P_L, (kW)	55.88	58.51	57.06	56.58	56.30	58.77	56.99	55.51	57.33	57.18	57.64	57.01
%MR	−0.3905	−0.7449	−0.4915	−1.1597	−0.6402	−0.1447	−0.4603	−0.5888	−0.6973	−0.4448	−1.3562	−0.7979

Table 11 shows the comparative statement of various techniques available in the literature for network reconfiguration and DG allocation. The test results show that the optimal configuration and DG allocation are found to be different using different techniques with the marginal difference between the power losses in the resulting configuration. Conversely, the proposed approach is demonstrated for the coordinated operation of DG allocation and reconfiguration in the presence of ESS, as a load and source, exclusively. Here, it can be noticed that the existing approaches are tested for constant power load, i.e., LM-1, across all cases. In contrast, the proposed approach is tested for LM-1, LM-2, and LM-3, which are formulated using several load combinations in a practical scenario. On comparing the DG allocation and network reconfiguration without ESS, and for constant power load, the power loss in [28], using the TLBO approach, is found to be 58.08 kW with DG allocation as 1329 (8), 1172 (24), and 726 (31), which offers the total size of 3227 kW. On the other hand, under identical operating conditions, the power loss in the proposed approach is 58.10 kW with DG allocation as 890 (25), 856 (9), and 792 (31), which is in a total size of 2538 kW. Here, it can be noticed that the optimization, performed using existing approaches, may not yield energy-efficient operation during power delivery in the present competitive energy market scenario.

The results show that the integration of electric vehicles in the existing network affects the EEP when ESS works as a load and or source differently. Therefore, it further requires investigating the ideal location of EV stations before their installation because the location of ESS, as a load, may not offer the optimal results when ESS works as a source. Further, the proposed approach performs better with enhanced EEP in terms of voltage profile, loadability, power loss, DG size, and margin of reliability, which is beneficial for both utilities and customers.

Table 11. Comparison of different approaches for 3-DG allocation and power loss reduction.

Case/Methods	Configuration	EV Location	Power Loss (kW)	DG Size	DG Location
Base Configuration	33, 34, 35, 36, 37	–	202.67	–	–
Optimal configuration	7, 9, 14, 32, 37	–	139.5	–	–
DG allocation in base Configuration under,		–			
LM-1					
LM-2	33, 34, 35, 36, 37		78.25	652, 999, 656	14, 26, 32
LM-3			76.78	781, 991, 407	32, 7, 18
			69.72	970, 542, 505	29, 9, 14
DG allocation in optimal configuration under,					
LM-1		–			
LM-2	7, 9, 14, 32, 37		72.19	968, 780, 997	23, 16, 27
LM-3			75.05	419, 408, 653	6, 18, 28
			65.07	680, 828, 622	12, 7, 30
DG allocation and Reconfiguration under,					
LM-1		–			
LM-2	7, 13, 11, 36, 27		58.10	890, 856, 792	25, 9, 31
LM-3	7, 12, 10, 32, 25		56.39	984, 811, 754	25, 15, 31
	7, 12, 10, 31, 27		52.18	892, 967, 780	29, 9, 16
DG allocation and Reconfiguration with EVs as a load					
LM-1					
LM-2					
LM-3	9, 28, 31, 33, 34	18	55.64	933, 885, 990	15, 7, 30
	9, 14, 28, 30, 33	18	53.37	977, 699, 930	25, 17, 7
	9, 27, 30, 33, 34	18	54.99	957, 920, 741	25, 8, 18

Table 11. *Cont.*

Case/Methods	Configuration	EV Location	Power Loss (kW)	DG Size	DG Location
DG allocation and Reconfiguration with EVs as a source					
LM-1					
LM-2					
LM-3	10, 27, 30, 33, 34	32	54.94	904, 767, 833	18, 7, 29
	7, 10, 14, 28, 30	32	53.02	594, 831, 985	32, 22, 25
	10, 28, 31, 33, 34	32	55.88	878, 979, 714	16, 6, 31
Ref. [28]					
IPSO	33, 34, 9, 32, 28	–	59.63	557, 922, 931	18, 7, 30
TLBO	6,14, 10, 32, 37		58.08	1329, 1172, 726	8, 24, 31
PSO	7, 13, 11, 32, 27		59.37	1732, 809, 550	29, 16, 7
Jaya	33, 13, 9, 28, 30		58.49	801, 1215, 745	18, 25, 9
Ref. [29]	7, 14, 10, 31, 28	–	73.05	526, 559, 584	28, 31, 33
Ref. [30]	7, 9, 14, 17, 37	–	92.98	55, 151, 103	18, 31, 32

7. Conclusions

In this paper, the energy efficiency performance (EEP) of the distribution system is realized through passive energy boosters (PEBs) and active energy boosters (AEBs), exclusively and in coordination, during power delivery in the presence of energy storage devices (ESS). The electric vehicles are the movable ESS that can work as load or source and are considered a significant constituent of ESS. For load representation, several combinations of voltage-dependent loads are modeled using a random distribution function to show the contribution of different loading patterns under various operating conditions. Here, the optimization results are obtained using the harmony search algorithm for the 33-node radial distribution system. From the test results, it has been observed that the EEP of the distribution system varies differently under different load models in the base and optimal configurations. However, the variation in power loss is slight, using various optimization techniques, but other parameters, such as the voltage profile, loadability, and DG size, are found to be significantly varying. The test results show that the optimal location of EVs, as a load and source, is not the same and can affect the EEP differently.

Considering the present scenarios of the integration of EVs at different locations, this work performs optimization. The EEP of the power distribution system under consideration has improved significantly, and it is beneficial for both utilities and customers. This work emphasizes the technical aspects of a smart energy system; however, in the future, the impact of renewable energy resources and ESS on EEP needs to be considered with hourly loading patterns by developing a bidirectional communication framework for control and monitoring. The optimal location of EVs is realized when ESS works as a load or source independently, whereas the common location requires further investigations.

Author Contributions: Conceptualization, P.K. and S.N.; data curation, P.K., S.N. and I.A.; formal analysis, P.K. and S.N.; funding acquisition, P.K. and H.A.; methodology, P.K., S.N. and H.A.; project administration, I.A. and M.S.T.; resources, P.K. and H.A.; software, P.K. and H.A.; supervision, I.A. and M.S.T.; validation, I.A. and M.S.T.; visualization, I.A. and M.S.T.; writing—original draft, P.K. and S.N.; writing—review and editing, I.A. and M.S.T. and H.A. All authors have read and agreed to the published version of the manuscript.

References

1. Kumar, P.; Thanki, D.V.; Singh, S.; Nikolovski, S. A new framework for intensification of energy efficiency in commercial and residential use by imposing social, technical and environmental constraints. *Sustain. Cities Soc.* **2020**, *62*, 102400. [CrossRef]
2. Ali, I.; Thomas, M.S.; Kumar, P. Energy efficient reconfiguration for practical load combinations in distribution systems. *IET Gener. Transm. Distrib.* **2015**, *9*, 1051–1060. [CrossRef]
3. Kumar, P.; Ali, I.; Thomas, M.S.; Singh, S. Imposing voltage security and network radiality for reconfiguration of distribution systems using efficient heuristic and meta-heuristic approach. *IET Gener. Transm. Distrib.* **2017**, *11*, 2457–2467. [CrossRef]
4. Kumar, P.; Ali, I.; Thomas, M.S.; Singh, S. A coordinated framework of dg allocation and operating strategy in distribution system for configuration management under varying loading patterns. *Electr. Power Compon. Syst.* **2020**, *48*, 12–29. [CrossRef]
5. Wang, K.; Li, H.; Maharjan, S.; Zhang, Y.; Guo, S. Green energy scheduling for demand side management in the smart grid. *IEEE Trans. Green Commun. Netw.* **2018**, *2*, 596–611. [CrossRef]
6. Haseeb, M.; Kazmi, S.A.; Malik, M.M.; Ali, S.; Bukhari, S.B.; Shin, D.R. Multi objective based framework for energy management of smart micro-grid. *IEEE Access* **2020**, *8*, 220302–220319. [CrossRef]
7. Kumar, P.; Singh, S.; Ali, I.; Ustun, T.S. Handbook of Research on Power and Energy System Optimization. In *2018 IGI Global, Engineering Science Reference*; IGI Global: Hershey, PA, USA, 2018.
8. Cao, B.; Dong, W.; Lv, Z.; Gu, Y.; Singh, S.; Kumar, P. Hybrid microgrid many-objective sizing optimization with fuzzy decision. *IEEE Trans. Fuzzy Syst.* **2020**, *28*, 2702–2710. [CrossRef]
9. Zhang, K.; Yu, J.; Ren, Y. Demand side management of energy consumption in a photovoltaic integrated greenhouse. *Int. J. Electr. Power Energy Syst.* **2022**, *134*, 107433. [CrossRef]
10. Kumar, P.; Brar, G.S.; Singh, S.; Nikolovski, S.; Baghaee, H.R.; Balkić, Z. Perspectives and intensification of energy efficiency in commercial and residential buildings using strategic auditing and demand-side management. *Energies* **2019**, *12*, 4539. [CrossRef]
11. Asrari, A.; Wu, T.; Lotfifard, S. The impacts of distributed energy sources on distribution network reconfiguration. *IEEE Trans. Energy Convers.* **2016**, *31*, 606–613. [CrossRef]
12. Dorostkar, G.M.R.; Fotuhi, F.M.; Lehtonen, M.; Safdarian, A. Value of distribution network reconfiguration in presence of renewable energy resources. *IEEE Trans. Power Syst.* **2015**, *31*, 1879–1888. [CrossRef]
13. Kavousi, F.A.; Rostami, M.A.; Niknam, T. Reliability-oriented reconfiguration of vehicle-to-grid networks. *IEEE Trans. Ind. Inform.* **2015**, *11*, 682–691. [CrossRef]
14. Xing, H.; Sun, X. Distributed generation locating and sizing in active distribution network considering network reconfiguration. *IEEE Access* **2017**, *5*, 14768–14774. [CrossRef]
15. Fu, Y.Y.; Chiang, H.D. Toward optimal multiperiod network reconfiguration for increasing the hosting capacity of distribution networks. *IEEE Trans Power Deliv.* **2018**, *33*, 2294–2304. [CrossRef]
16. Azizivahed, A.; Arefi, A.; Ghavidel, S.; Shafie, K.M.; Li, L.; Zhang, J.; Catalão, J.P. Energy management strategy in dynamic distribution network reconfiguration considering renewable energy resources and storage. *IEEE Trans. Sustain. Energy* **2019**, *11*, 662–673. [CrossRef]
17. Liu, Y.; Li, J.; Wu, L. Coordinated optimal network reconfiguration and voltage regulator/DER control for unbalanced distribution systems. *IEEE Trans. Smart Grid* **2018**, *10*, 2912–2922. [CrossRef]
18. Song, Y.; Zheng, Y.; Liu, T.; Lei, S.; Hill, D.J. A new formulation of distribution network reconfiguration for reducing the voltage volatility induced by distributed generation. *IEEE Trans. Power Syst.* **2019**, *35*, 496–507. [CrossRef]
19. Nick, M.; Cherkaoui, R.; Paolone, M. Optimal planning of distributed energy storage systems in active distribution networks embedding grid reconfiguration. *IEEE Trans. Power Syst.* **2017**, *33*, 1577–1590. [CrossRef]
20. Naguib, M.; Omran, W.A.; Talaat, H.E. Performance Enhancement of Distribution Systems via Distribution Network Reconfiguration and Distributed Generator Allocation Considering Uncertain Environment. *J. Mod. Power Syst. Clean Energy* **2021**, *10*, 647–655. [CrossRef]
21. Cattani, I.B.; Chaparro, E.; Barán, B. Distribution system operation and expansion planning using network reconfiguration. *IEEE Lat. Am. Trans.* **2020**, *18*, 845–852. [CrossRef]
22. Ahmed, H.M.; Salama, M.M. Energy management of AC–DC hybrid distribution systems considering network reconfiguration. *IEEE Trans. Power Syst.* **2019**, *34*, 4583–4594. [CrossRef]
23. Takenobu, Y.; Yasuda, N.; Kawano, S.; Minato, S.I.; Hayashi, Y. Evaluation of annual energy loss reduction based on reconfiguration scheduling. *IEEE Trans. Smart Grid* **2016**, *9*, 1986–1996. [CrossRef]
24. Asrari, A.; Ansari, M.; Khazaei, J.; Fajri, P.; Amini, M.H.; Ramos, B. The impacts of a decision making framework on distribution network reconfiguration. *IEEE Trans. Sustain. Energy* **2020**, *12*, 634–645. [CrossRef]
25. Huang, W.; Zheng, W.; Hill, D.J. Distribution network reconfiguration for short-term voltage stability enhancement: An efficient deep learning approach. *IEEE Trans. Smart Grid* **2021**, *12*, 5385–5395. [CrossRef]
26. Zhan, J.; Liu, W.; Chung, C.Y.; Yang, J. Switch opening and exchange method for stochastic distribution network reconfiguration. *IEEE Trans. Smart Grid* **2020**, *11*, 2995–3007. [CrossRef]
27. Gao, H.; Ma, W.; Xiang, Y.; Tang, Z.; Xu, X.; Pan, H.; Zhang, F.; Liu, J. Multi-Objective Dynamic Reconfiguration for Urban Distribution Network Considering Multi-Level Switching Modes. *J. Mod. Power Syst. Clean Energy* **2021**, 1–14. [CrossRef]

28. Rawat, M.S.; Vadhera, S. Heuristic optimization techniques for voltage stability enhancement of radial distribution network with simultaneous consideration of network reconfiguration and DG sizing and allocations. *Turk. J. Electr. Eng. Comput. Sci.* **2019**, *27*, 330–345. [CrossRef]
29. Rao, R.S.; Ravindra, K.; Satish, K.; Narasimham, S.V. Power loss minimization in distribution system using network reconfiguration in the presence of distributed generation. *IEEE Trans. Power Syst.* **2012**, *28*, 317–325. [CrossRef]
30. Esmaeilian, H.R.; Fadaeinedjad, R. Energy loss minimization in distribution systems utilizing an enhanced reconfiguration method integrating distributed generation. *IEEE Syst. J.* **2014**, *9*, 1430–1439. [CrossRef]
31. Wang, B.; Zhang, C.; Dong, Z.Y. Interval optimization based coordination of demand response and battery energy storage system considering SoC management in a microgrid. *IEEE Trans. Sustain. Energy* **2020**, *11*, 2922–2931. [CrossRef]
32. Diab, A.A.; Sultan, H.M.; Mohamed, I.S.; Kuznetsov, O.N.; Do, T.D. Application of different optimization algorithms for optimal sizing of PV/wind/diesel/battery storage stand-alone hybrid microgrid. *IEEE Access* **2019**, *7*, 119223–119245. [CrossRef]
33. Islam, M.M.; Nagrial, M.; Rizk, J.; Hellany, A. Dual stage microgrid energy resource optimization strategy considering renewable and battery storage systems. *Int. J. Energy Res.* **2021**, *45*, 21340–21364. [CrossRef]
34. Faisal, M.; Hannan, M.A.; Ker, P.J.; Hussain, A.; Mansor, M.B.; Blaabjerg, F. Review of energy storage system technologies in microgrid applications: Issues and challenges. *IEEE Access* **2018**, *6*, 35143–35164. [CrossRef]
35. Kumar, P.; Ali, I.; Thomas, M.S. Energy efficiency analysis of reconfigured distribution system for practical loads. *Perspect. Sci.* **2016**, *8*, 498–501. [CrossRef]
36. Geem, Z.W.; Kim, J.H.; Loganathan, G.V. A new heuristic optimization algorithm: Harmony search. *Simulation* **2001**, *76*, 60–68. [CrossRef]
37. Dubey, M.; Kumar, V.; Kaur, M.; Dao, T.P. A systematic review on harmony search algorithm: Theory, literature, and applications. *Math. Probl. Eng.* **2021**, *2021*, 5594267. [CrossRef]
38. Ala'a, A.; Alsewari, A.A.; Alamri, H.S.; Zamli, K.Z. Comprehensive review of the development of the harmony search algorithm and its applications. *IEEE Access* **2019**, *7*, 14233–14245.